

Crawling Waves from Radiation Force Excitation

GAEGYOO HAH,¹ CHRISTOPHER HAZARD,^{PHD TO PHER}

University of Rochester

. N 1 t Y 4 e . 6 f 2 7

restrictions on the Doppler pulse repetition frequency. Equally important, the creation of crawling waves from opposing shear sources sets up a quasiplane strain condition with the dominant displacement approximately di

where D is the distance between the vibration source.

Eq. (2) shows that the square of the vibration amplitude has a hyperbolic cosine term that accounts for the atten

where the slow time shift is found to be $t = 2kx/c$. The shear speed can be estimated to be

Both Eqs. (4) and (6) can be modified for cases where the phase difference is continuous or stepped rather than the frequency difference generates crawling waves, i.e. with

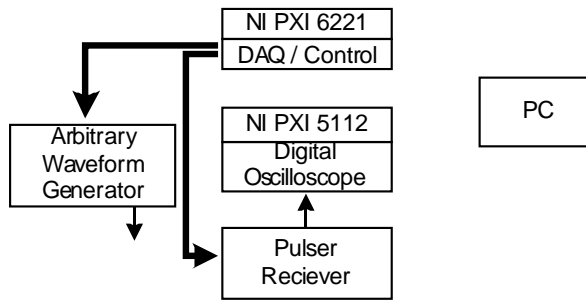
where ϕ is changing. In this case each frame of the movie is independent and Eq. (4) still applies because Eq. (4) is derived for a fixed frame. Eq. (6) would be modified to be

where ϕ is the phase difference measured between the crawling waves at x and $x + \Delta x$.

These derivations assume that vibrations of sources are continuous and sinusoidal. This is typically the case with applications by mechanical sources. In applications employing radiation force the 'pushing' beam can only apply force unidirectionally, not bidirectionally as in the case of mechanical transducers. Furthermore, in most ultrasound systems, it is desirable to only acquire pulse echo tracking while the pushing beam is off, due to strong interference effects. As a result, the vibrations at each point of the medium will be pulse-shaped rather than sinusoidal and some processing of the measured data is needed to be able to use Eq. (4) and (8) for local shear speed estimations. This will be discussed in the next section.

III EXPERIMENTS AND DISCUSSION

If we assume that the system shown in figure 2 is a linear system where the input is the electric-excitation signal and the output is the shear displacements, then the system will ideally show both linearity and shift-invariance as



where $f(t)$ is the excitation signal for the left-side source, $g(t)$ is the excitation signal for the right-side source, $F(t)$ is the displacement due to $f(t)$, $G(t)$ is the displacement due to $g(t)$, is

the delay and $L[\]$ means the system response. Physically, the linearity will hold for small-strain assumptions; if larger strains were induced, then the system would behave in a more hyperelastic manner that would be nonlinear. In this section, we first show experimental proof for Eq. (9) and then use the property to process the data to generate crawling waves.

III.1 Experimental setup

The experimental setup shown in figure 3 is used. The setup consists of two single element 5 MHz focused transducers (Data, focal depth 2 in, diameter 0.75 in) used for radiation-force excitation, one single element 5 MHz scan transducer (Data, focal depth 2 in, diameter 0.375 in) for pulse-echo measurements, control system (National Instrument NI PXI 1033), pulse/receiver (JSR DPR 300), dual-channel arbitrary-function generator (Tektronix AFG 3022B), broadband power amplifier (Electronics & Innovation A 075) and an xyztable (Velmex, UniSlide). The control system has three modules DAQ (Data Acquisition, NI PXI 6221), DSO (Digital Oscilloscope, NI PXI 5112) and AWG (Arbitrary Waveform Generator, NI PXI 5412). A matching circuit is built between the power-amplifier and the transducers.

FIG. 6 Processed results of experimental data. (a) To examine the lateral profile, we took a line A at a fixed depth of 3.75 cm from the surface.

Three separate experiments are done under identical experimental conditions: exciting left side source only, right side source only and both source simultaneously.

III.2 Experimental results

The displacement of the phantom is calculated through several pro er

Spatial-domain smoothing can be done either with a two-dimensional median filter or with smoothing in axial and lateral directions, where the axial direction is filtered first because it is more slowly varying than the lateral profile. Time-domain smoothing, on the other hand, identifies the expected rise and fall of a propagating wave in the form of a motion filter and removes drifts and other artifacts. The results are shown in figure 6. Typical displacements are below 3 μm . Instead of showing all the frames, we will focus on the lateral profile at a fixed depth of 3.75 cm from the top, shown as line A of figure 6 (a). Figures 6 (b) to (e) show displacement profiles due to the left-side source only, right-side source only and both sources at 5.4, 6.68, 7.96 and 9.56 ms after the onset of the excitation pulses respectively. We observe good correspondence in these graphs despite some minor discrepancies. The match is more easily seen in figures 6 (f) to (h), where the images of a plane defined in figure 6 (a) as a frame-lateral dimension image with time on the vertical axis, are shown, respectively, for cases of the left-side push only, the right-side push only and simultaneous push of left and right side sources. Further analysis of the image reveals that the shear wave speed is about 1.8 m/s. Also thermal heating is measured at below 2°C.

III.3 Generation of crawling interference pattern

Let

A Logiq 9 (GE) system has been modified to implement the above-mentioned functionality. A transrectal probe capable of forming focuses at 2.5 cm deep and 18 mm apart is installed in the system. Detailed information and experiments thereof will be covered in a separate paper.

IV CONCLUSION

Crawling waves can be generated using acoustic radiation-force excitation and imaged with pulse-echo sequences for analysis of the underlying elastic properties. However, there are practical differences between those crawling waves produced by mechanical vibration sources and those produced by radiation-force excitation. Mechanical sources can be bidirectional, whereas radiation force sources can only push in the direction of the propagating beam. The simplest approximation to a sinusoidal mechanical vibration source would be a radiation force pulse that is on for 50% and off for 50% of the cycle. However, because of the strong interference between the pushing excitation and the tracking pulses, there is a need to balance the timing sequence between pushing and tracking. Furthermore, transducer heating can also limit the time or duty cycle that can be devoted to the radiation-force excitation. Thus, radiation force excitations will have a limited duty cycle in the time domain. If the beams are highly focused, the source of vibration will be highly localized in the spatial domain as well. Because of these factors, the interference peaks will be shorter in time and space as compared to the case of purely sinusoidal excitation. This, in turn, may require higher sampling rates, spatially and temporally, in order to accurately track the interference peaks. Another limitation of radiation force excitation is in the relatively low (μm range) displacements that are effected with conventional imaging transducers and FDA limits. Nonetheless, some clinical targets that are deep or relatively inaccessible to compressor or vibration sources, may be excited with crawling waves generated

7. Zhang M, Castaneda B